

# Conformational Properties of Boron-Bridged Dimethylethylenediamino Bis(boratabenzene) Zirconium(IV) and Iron(II) Complexes

Arthur J. Ashe III,\* Saleem Al-Ahmad, Xiangdong Fang, and Jeff W. Kampf

Department of Chemistry, University of Michigan, Ann Arbor, Michigan 48109-1055

Received October 10, 2000

The reaction of 1-chloro-1-boracyclohexadiene (**12**) with *N,N*-dimethyl-*N,N*-bis(trimethylsilyl)ethylene-1,2-diamine followed by LDA afforded the dilithium salt of *N,N*-bis(1-boratabenzene)-*N,N*-dimethylethylene-1,2-diamine (**14**). The reaction of **14** with  $ZrCl_4$  afforded the boron-bridged dimethylethylenediamino bis(boratabenzene) zirconium dichloride complex **8**, while reaction of **14** with  $FeCl_2$  afforded the corresponding dimethylethylenediamino-bridged iron(II) complex **9**. The structures of **8** and **9** were determined by X-ray diffraction. In each case the boratabenzene units are bridged by an approximately  $C_2$ -symmetric dimethylethylenediamino bridge which makes **8** and **9** chiral. A barrier to interconversion of the enantiomeric conformers of **8** was determined by 2D  $^1H$  NOESY as  $21.2 \pm 0.2$  kcal/mol, while the corresponding barrier of **9** was determined from variable-temperature  $^{13}C$  NMR spectroscopy to be  $16.9 \pm 0.5$  kcal/mol. Both barriers involve rotation about the exocyclic B–N  $\pi$ -bonds. Comparison has been made with the corresponding bridged cyclopentadienyl complexes **10** and **11**.

## Introduction

Bridged or *ansa*-metallocenes are well-known for both the ferrocene<sup>1–4</sup> and bent metallocene<sup>5–8</sup> types of structures. For both kinds of structures a small bridging group constrains the rings, thereby opening the wedge between the rings so that the metal is more accessible. The bridge also restrains the rotation about the ring–metal axis, thereby limiting the conformational mobility. Much recent attention has focused on the bent *ansa*-metallocenes derived from the group 4 metals, since many of these compounds are highly active and stereoselective catalysts toward polymerization of olefins.<sup>9</sup>

Boratabenzenes can serve as surrogates for Cp in a variety of important organometallic compounds.<sup>10,11</sup> For example, bis(boratabenzene)iron complexes, e.g. **1** (Chart 1), have ferrocene-like properties.<sup>12,13</sup> Similarly, analogous zirconium complexes of boratabenzene **2** and cyclopentadienyl **4** have been converted to olefin polymerization catalysts with nearly identical activities.<sup>14,15</sup> For these reasons we examined bridged bis(boratabenzene)zirconium complexes **5** and **6**, which have structures closely analogous to the corresponding *ansa*-

(1) (a) Long, N. J. *Metallocenes*; Blackwell Science: Oxford, U.K., 1998; pp 184–195. (b) Herberhold, M. *Ferrocene Compounds Containing Heteroatoms*. In *Ferrocenes*; Togni, A., Hayashi, T., Eds.; VCH: Weinheim, Germany, 1995; pp 254–264.

(2) (a) Osborne, A. G.; Whiteley, R. H. *J. Organomet. Chem.* **1975**, *101*, C27. (b) Stoeckli-Evans, H.; Osborne, A. G.; Whiteley, R. H. *Helv. Chim. Acta* **1976**, *59*, 2402; **1977**, *16*, 624. (c) Foucher, D. A.; Tang, B.-Z.; Mannes, I. *J. Am. Chem. Soc.* **1992**, *114*, 6246. (d) Dement'ev, V. V.; Cervantes-Lee, F.; Parkanyi, L.; Sharma, H.; Pannell, K. H.; Nguyen, M. T.; Diaz, A. *Organometallics* **1993**, *12*, 1983.

(3) (a) Seyferth, D.; Withers, H. P., Jr. *Organometallics* **1982**, *1*, 1275. (b) Osborne, A. G.; Whiteley, R. H.; Meads, R. E. *J. Organomet. Chem.* **1980**, *193*, 345. (c) Stoeckli-Evans, H.; Osborne, A. G.; Whiteley, R. H. *J. Organomet. Chem.* **1980**, *194*, 91.

(4) (a) Davison, A.; Smart, J. C. *J. Organomet. Chem.* **1969**, *19*, P7; **1979**, *174*, 321. (b) Abel, E. W.; Booth, M.; Orrell, K. G. *J. Organomet. Chem.* **1981**, *208*, 213. (c) Johnston, E. R.; Brandt, P. F. *Organometallics* **1998**, *17*, 1460.

(5) (a) Halterman, R. L. *Chem. Rev.* **1992**, *92*, 965. (b) Ryan, E. J. In *Comprehensive Organometallic Chemistry II*; Lappert, M. F., Ed.; Pergamon: Oxford, U.K., 1995; Vol. 4, p 483.

(6) (a) Wild, F. R. W. P.; Zsolnai, L.; Huttner, G.; Brintzinger, H. H. *J. Organomet. Chem.* **1982**, *232*, 233. (b) Ewen, J. A. *J. Am. Chem. Soc.* **1984**, *106*, 6355. (c) Kaminsky, W.; K lper, K.; Brintzinger, H. H.; Wild, F. R. W. P. *Angew. Chem., Int. Ed. Engl.* **1985**, *24*, 507.

(7) (a) Katz, T. J.; Acton, N. *Tetrahedron Lett.* **1970**, 2497. (b) Smith, J. A.; von Seyerl, J.; Huttner, G.; Brintzinger, H. H. *J. Organomet. Chem.* **1979**, *173*, 175.

(8) Wiesenfeldt, H.; Reimuth, A.; Barsties, E.; Evertz, K.; Brintzinger, H. H. *J. Organomet. Chem.* **1989**, *369*, 359.

(9) For recent reviews, see: (a) Brintzinger, H. H.; Fischer, D.; M lhaupt, R.; Rieger, B.; Waymouth, R. M. *Angew. Chem., Int. Ed. Engl.* **1995**, *34*, 1143. (b) *Ziegler Catalysts*; Fink, G., M lhaupt, R., Brintzinger, H. H., Eds.; Springer-Verlag: Berlin, Germany, 1995. (c) Coates, G. W.; Waymouth, R. M. In *Comprehensive Organometallic Chemistry II*; Hegedus, L. S., Ed.; Pergamon: Oxford, U.K., 1995; Vol. 12, p 1193. (d) Aulbach, M.; K ber, F. *Chem. Unserer Zeit* **1994**, *28*, 197. (e) Janiak, C. *Metallocene Catalysts for Olefin Polymerization*. In *Metallocenes*; Togni, A., Haltermann, R. L., Eds.; Wiley-VCH: Weinheim, Germany, 1998; Vol. 2, pp 547–623. (f) Gladysz, J. A. *Chem. Rev.* **2000**, *100*, 1167–1682.

(10) (a) Herberich, G. E. In *Comprehensive Organometallic Chemistry*; Wilkinson, G., Stone, F. G. A., Abel, E. W., Eds.; Pergamon Press: Oxford, U.K. 1982; Vol. 1, p 381. (b) Herberich, G. E.; Ohst, H. *Adv. Organomet. Chem.* **1986**, *25*, 199. (c) Herberich, G. E. In *Comprehensive Organometallic Chemistry II*; Housecroft, C. E., Ed.; Pergamon: Oxford, U.K., 1995; Vol. 1 p 197.

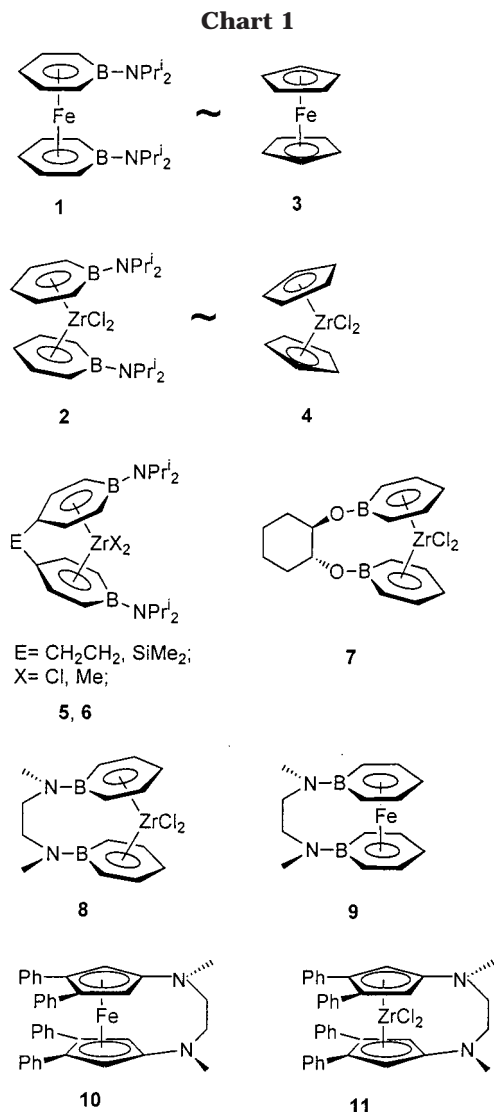
(11) For recent work on boratabenzenes see: (a) Herberich, G. E.; Englert, U.; Ganter, B.; Pons, M. *Eur. J. Inorg. Chem.* **2000**, 5, 979. (b) Hoic, D. A.; DiMare, M.; Fu, G. C. *J. Am. Chem. Soc.* **1997**, *119*, 7155. Tweddell, J.; Hoic, D. A.; Fu, G. C. *J. Org. Chem.* **1997**, *62*, 8286. (c) Ashe, A. J., III; Fang, X.; Kampf, J. W. *Organometallics* **1999**, *18*, 1365. (d) Lee, B. Y.; Bazan, G. C. *J. Am. Chem. Soc.* **2000**, *122*, 8577.

(12) Ashe, A. J., III; Meyers, E.; Shu, P.; Von Lehmann, T.; Bastide, J. *J. Am. Chem. Soc.* **1975**, *97*, 6865.

(13) Ashe, A. J., III; Kampf, J. W.; M ller, C.; Schneider, M. *Organometallics* **1996**, *15*, 387.

(14) Bazan, G. C.; Rodriguez, G.; Ashe, A. J., III; Al-Ahmad, S.; M ller, C. *J. Am. Chem. Soc.* **1996**, *118*, 2291.

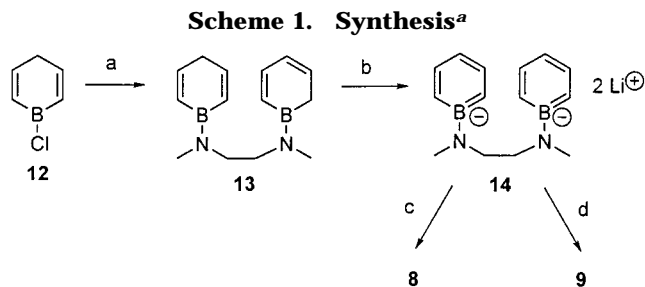
(15) For recent work related work see: (a) Bazan, G. C.; Rodriguez, G.; Ashe, A. J., III; Al-Ahmad, S.; Kampf, J. W. *Organometallics* **1997**, *16*, 2492. (b) Rogers, J. S.; Bazan, G. C.; Sperry, C. K. *J. Am. Chem. Soc.* **1997**, *119*, 9305.



zirconocenes.<sup>16</sup> To explore structurally more diverse bridged boratabenzene complexes, we have now prepared the dimethylethylenediamino bridged boratabenzene zirconium and iron complexes **8** and **9**, respectively. These are compared with the bridged Cp complexes **10**<sup>17</sup> and **11**<sup>18</sup> reported by Plenio.

### Results and Discussion

1-Aminoboratabenzenes are generally prepared by reaction of 1-chloro-1-boracyclohexadiene (**12**) with the appropriate amine followed by deprotonation.<sup>13</sup> We find that the reaction of **12** with *N,N*-dimethyl-*N,N*-bis-(trimethylsilyl)-1,2-diaminoethane<sup>19</sup> gives a 96% yield of **13** (Scheme 1). The NMR spectra of **13** indicate that it exists as a mixture of double-bond isomers. No attempt was made to separate these isomers, and the mixture was converted to the dilithium salt **14** by reaction of LDA in THF. The <sup>1</sup>H, <sup>11</sup>B, and <sup>13</sup>C NMR spectra of **14** show a typical boratabenzene pattern.<sup>20</sup> Reaction of **14** with ZrCl<sub>4</sub> in ether gave **8** as red crystals,



<sup>a</sup> Key: (a) 1/2 Me(Me<sub>3</sub>Si)NCH<sub>2</sub>CH<sub>2</sub>N(SiMe<sub>3</sub>)Me; (b) LDA; (c) ZrCl<sub>4</sub>; (d) FeCl<sub>2</sub>.

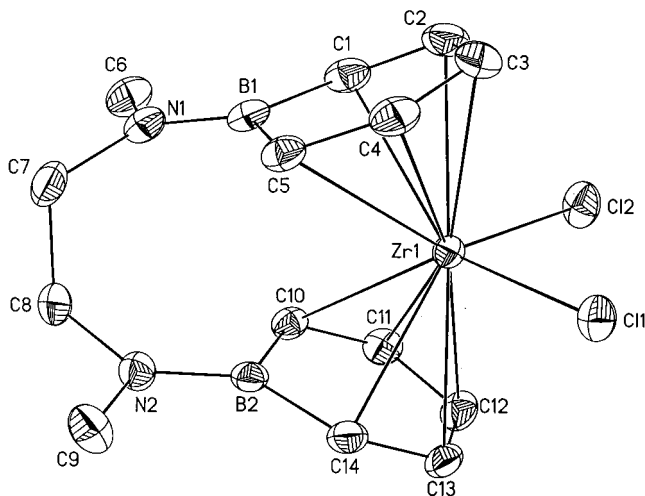


**Figure 1.** Molecular structure and atom labeling for **8**.

**Table 1. Comparison of Selected Average Distances (Å) and Angles (deg) for **2**, **8**, and **9****

	<b>2</b>	<b>8</b>	<b>9</b>
Distances			
M–B <sup>a</sup>	2.980(2)	2.893(3)	2.303(5)
M–C <sub>α</sub> <sup>b</sup>	2.67(2)	2.63(3)	2.138(5)
M–C <sub>β</sub> <sup>b</sup>	2.57(2)	2.573(5)	2.104(16)
M–C <sub>γ</sub> <sup>b</sup>	2.483(5)	2.522(2)	2.094(6)
B–N	1.396(6)	1.413(4)	1.435(7)
B–C <sub>α</sub>	1.552(7)	1.547(3)	1.544(7)
C <sub>α</sub> –C <sub>β</sub>	1.379(7)	1.391(5)	1.409(7)
C <sub>β</sub> –C <sub>γ</sub>	1.403(7)	1.411(10)	1.414(7)
PLC5–B <sup>c</sup>	0.22(1)	0.22(1)	0.10(1)
Angles			
PLC5/PLC5'	50.4	49.2	9.3

<sup>a</sup> M = Zr for **2** and **8**; M = Fe for **9**. <sup>b</sup> C<sub>α</sub>, C<sub>β</sub>, and C<sub>γ</sub> designate the carbon atoms of the boratabenzene rings which are at 1,2-, 1,3-, or 1,4-positions to the boron atom, respectively. <sup>c</sup> PLC5 refers to the plane defined by the five carbon atoms of the boratabenzene.

which could be recrystallized from toluene. In a similar manner reaction of **14** with FeCl<sub>2</sub> gave **9** as a dark red crystalline solid which was recrystallized from pentane/dichloromethane. Structures were obtained for both metal complexes by single-crystal X-ray diffraction.

The molecular structure of **8** is illustrated in Figure 1, while selected bond distances are collected in Table 1. This structure resembles that of the *trans*-1,2-cyclohexanedioxy-bridged zirconium complex **7**, recently reported by Bazan.<sup>21</sup> It is useful to compare the structure of **8** with that of its nonbridged relative **2**.<sup>14</sup> The

(16) Ashe, A. J., III; Al-Ahmad, S.; Fang, X.; Kampf, J. W. *Organometallics* **1998**, *17*, 3883.

(17) Plenio, H.; Burth, D. *J. Organomet. Chem.* **1996**, *519*, 269.

(18) Plenio, H.; Burth, D. *Angew. Chem., Int. Ed. Engl.* **1995**, *34*, 800. Plenio, H.; Burth, D. *Organometallics* **1996**, *15*, 4054.

(19) Skorini, S. J.; Senning, A. *Tetrahedron* **1980**, *36*, 539.

(20) Herberich, G. E.; Schmidt, B.; Englert, U. *Organometallics* **1995**, *14*, 471.

(21) Rogers, J. S.; Lachicotte, R. J.; Bazan, G. C. *J. Am. Chem. Soc.* **1999**, *121*, 1288.

geometries of the dialkylaminoboratabenzene units of **8** and **2** are very similar. The corresponding intraligand C–C, B–C, and B–N distances vary by no more than 0.02 Å. Thus, the geometry of the boratabenzene unit of **8** is little affected by the bridging.

The major difference between structures **8** and **2** is the juxtaposition of the dialkylamino groups relative to the metallocene wedge. The diisopropylamino groups of **2** are disposed at  $C_2$ -related positions at the front side of the open wedge. On the other hand, the dimethylethylenediamino bridge of **8** spans the shorter gap at the backside of the wedge. This bridge is symmetrical, which gives the molecule **8** an approximate  $C_2$  axis bisecting the  $ZrCl_2$  unit.

As has been previously discussed, the Zr atom of **2** is slip-distorted away from the boron atoms so that the B–Zr distance (2.98 Å) is too long for strong bonding.<sup>14</sup> For **8** the slip distortion is less pronounced, with B–Zr distances of 2.907(2) and 2.879(2) Å. However, in both molecules the Zr is more strongly bound to the five coplanar carbon atoms of each ring. The boron atoms are displaced out of these planes away from the metal by 0.22(1) Å (average) in both cases. These  $sp^2$ -hybridized B atoms are strongly  $\pi$ -bound to their pendant  $sp^2$ -hybridized N atoms (B–N = 1.396(6) Å for **2** and 1.413(2) Å for **8**).

The bridging of **8** takes place with very little distortion. The planes made by the five carbon atoms of each ring of **2** intersect at 50.4(2)°, while the corresponding planes of **8** intersect at 49.2(1)°. Finally the torsional angle in the bridge of **8** (N(1)C(7)C(8)/C(7)C(8)N(2) = 75.3(2)°) indicates that it is close to staggered and relatively strain free.

The <sup>1</sup>H NMR spectrum of **8** in  $C_6D_6$  at 25 °C exhibits five nonequivalent boratabenzene signals ( $\delta$  7.75, 6.93, 6.38, 5.73, 4.82), which is consistent with the chiral environment present in the crystallographic conformation. In contrast, the <sup>1</sup>H NMR spectrum of **2** in  $C_6D_6$  at 25 °C exhibits only three boratabenzene signals ( $\delta$  5.70, 5.84, 7.14) in the ratio of 2:1:2, which is consistent with an averaged achiral environment. Assuming that **2** also populates its chiral crystallographic conformation in solution, a rapid interconversion of the enantiomers by relative rotation about the Zr–ring axis is indicated. This proposal is very plausible, since similar conformational equilibration is usually fast for group 4 bent metallocenes.<sup>22</sup> In the case of **8** rotation about the Zr–ring axis must be hindered by the rigid bridge.

When the temperature is raised to 110 °C, the nonequivalent signals for the boratabenzene ring protons of **8** broaden but do not coalesce. However, exchange between the two enantiomeric conformations of **8** could be demonstrated using <sup>1</sup>H NOESY spectroscopy. Large positive chemical exchange cross-peaks were observed for the signals  $\delta$  7.75 and 6.93, assigned to H(1)=H(14) and H(5)=H(10), and  $\delta$  5.73 and 4.82, assigned to H(2)=H(13) and H(4)=H(11). The rate constant for chemical exchange is a function of volumes of the diagonal and cross-peaks and the mixing times in the NOESY experiment. Using the method derived by Ernst and co-workers<sup>23</sup>  $\Delta G^\ddagger$  for exchange was evaluated as 21.3  $\pm$  0.2 kcal/mol at 45 °C (Table 2).

**Table 2. Barriers to Conformation Equilibration of Aminoboratabenzene and Aminocyclopentadienyl Metal Complexes**

compd	$\Delta G^\ddagger$ (kcal/mol)	$T$ (°C)
Iron(II) Complexes		
$[C_5H_5BN(i-Pr)_2]_2Fe$ ( <b>1</b> ) <sup>a</sup>	14.8	25
$(MeNCH_2CH_2NMe)[1-C_5H_5B]_2Fe$ ( <b>9</b> ) <sup>b</sup>	16.9	75
$(MeNCH_2CH_2NMe)[3,4-Ph_2C_5H_2]_2Fe$ ( <b>10</b> ) <sup>b</sup>	10.0	–60
Zirconium(IV) Dichloride Complexes		
$[C_5H_5BN(i-Pr)_2]ZrCl_2$ ( <b>2</b> ) <sup>c</sup>	18.2	62
$(MeNCH_2CH_2NMe)[1-C_5H_5B]_2ZrCl_2$ ( <b>8</b> ) <sup>b</sup>	21.3	45
$(MeNCH_2CH_2NMe)[3,4-Ph_2C_5H_2]_2ZrCl_2$ ( <b>11</b> ) <sup>b</sup>	13.0	10
<i>meso</i> -[1-C <sub>4</sub> H <sub>8</sub> N-3-Ph-C <sub>5</sub> H <sub>3</sub> ] <sub>2</sub> ZrCl <sub>2</sub> ( <b>16</b> ) <sup>d</sup>	12.1	–25

<sup>a</sup> Reference 13. <sup>b</sup> This work. <sup>c</sup> Reference 14. <sup>d</sup> Reference 27.

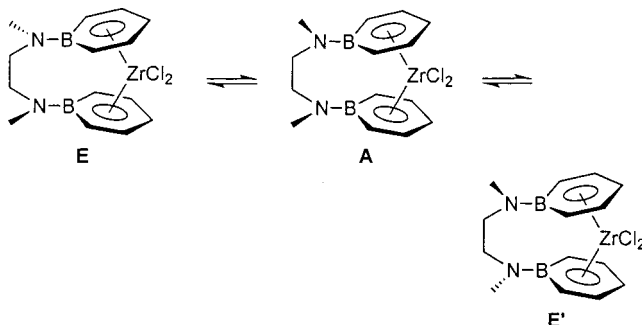


**Figure 2.** Schematic representation of the interconversion of the enantiomeric conformations (**E**, **E'**) of **8** via an unobserved achiral conformer (**A**).

The interconversion of the enantiomeric conformations (**E**, **E'**) of **8**, schematically illustrated in Figure 2, involves a small rotation about the Zr–ring axis together with a reversal of the BN(Me)CH<sub>2</sub>CH<sub>2</sub>N(Me)B bridge. We propose that reversal of the bridge takes place by a 180° rotation about one of the B–N  $\pi$  bonds to an unobserved achiral conformation (**A**), followed by another 180° rotation in the opposite direction about the second B–N  $\pi$  bond<sup>24</sup> (**E** = **A** = **E'**). For comparison, the barrier to B–N bond rotation of **2** in  $C_6D_6$  at 62 °C has been measured as  $\Delta G^\ddagger = 18.2 \pm 0.5$  kcal/mol.<sup>14</sup> Thus, the major component of the conformational equilibrium of **8** is plausibly assigned to rotation about the B–N bonds.

The molecular structure of **9** is illustrated in Figure 3, while selected bond distances are collected in Table 1. The structure of **9** shows a ferrocene-like arrangement in which the iron atom is sandwiched between two dimethylethylenediamino-bridged boratabenzene rings.

Although the structure of **1** has not been determined, comparison can be made with a number of available structures of other late-transition-metal boratabenzene complexes.<sup>10</sup> Comparison of the dialkylaminoboratabenzene complexes **9** and **15** seems particularly relevant.<sup>13</sup> This comparison indicates that neither the geometry of the dialkylaminoboratabenzene rings of **9** nor the metal–ligand distances are extraordinary. The iron atom of **9** shows only a small slip distortion away from the boron atoms, so that the aminoboratabenzene ligands are  $\eta^6$ -coordinated. Although the metal bonding to carbon is stronger than to boron, this difference is smaller than is found for **8**. The exocyclic B–N bonds

(22) Coates, G. W.; Waymouth, R. M. *Science* **1995**, *267*, 217.

(23) Jeener, J.; Meier, B. H.; Bachmann, P.; Ernst, R. R. *J. Chem. Phys.* **1979**, *71*, 4546.

(24) This proposal is formally similar to the mechanism proposed for bridge reversal in [3]-triheteroferrocenes.<sup>4b</sup>

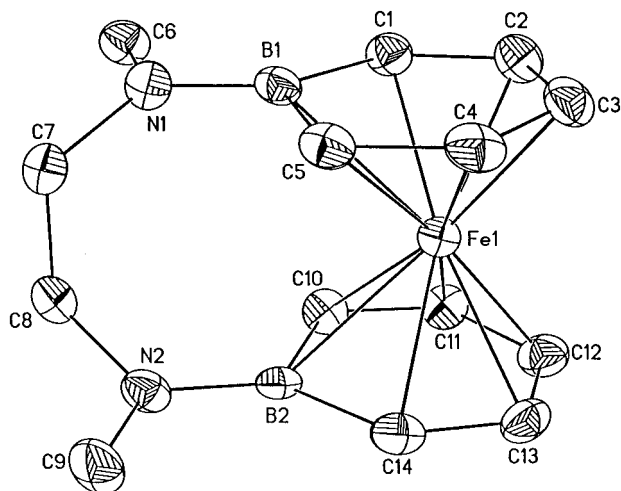


**Figure 3.** Molecular structure and atom labeling for **9**.

of **9** (1.443(7), 1.427(6) Å) are also longer than those found for **8** (1.413(2) Å). These differences can probably be ascribed to the smaller electron withdrawal by Fe(II) relative to Zr(IV).

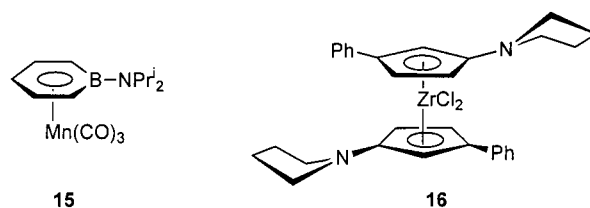
The dimethylethylenediamino bridge of **9** resembles the bridge of **8**. This symmetrical bridge also gives **9** an apparent  $C_2$  axis which passes through the metal atom. However the bridge of **9** seems to cause more distortion than in **8**. The nitrogen atoms of the bridge are slightly pyramidalized (sum of angles: at N(1), 356.7°; at N(2), 356.4°). The planes of the five carbon atoms of each ring are not parallel, as expected for a strain-free structure, but are tilted by 9.8°.

The  $^{13}\text{C}$  NMR spectrum of **9** in  $\text{C}_6\text{D}_6$  at 25 °C shows five nonequivalent boratabenzene signals ( $\delta$  92.1, 89.4, 73.9, 71.6, 65.9), which indicate that the CH groups  $\alpha$  and  $\beta$  to boron are diastereotopic. In contrast, the  $^{13}\text{C}$  NMR spectrum of **1** at 25 °C shows only one signal each for the  $\alpha$ -carbons ( $\delta$  64.5) and  $\beta$ -carbons ( $\delta$  92.8). Thus, the nonbridged **1** shows rapid rotation about the ring–metal axis, while the rotation is restricted in the bridged complex **9** in a manner similar to that of **8**. The barrier to conformational interconversion in **9** was evaluated by observing the coalescence of the signals for the diastereotopic  $\beta$ -carbons ( $\delta$  92.1, 89.4). Coalescence at 75 °C gave  $\Delta G^\ddagger = 16.9 \pm 0.5$  kcal/mol.

The interconversion of the enantiomeric conformations of **9** seems completely analogous to that of **8**. Again, we propose that the major component of the conformational equilibration is the rotation about the B–N bonds. For comparison the barrier to B–N rotation of **1** has been measured as 14.8 kcal/mol at 25 °C.<sup>13</sup>

It is particularly interesting to compare boratabenzene complex **9** with the corresponding ferrocene complex **10**, which has been investigated by Plenio.<sup>18</sup> The crystal structure of **10** shows a conformation which is closely analogous to that of **9**. The dimethylethylenediamino bridge gives **10** an approximate  $C_2$  symmetry. The planes of the two Cp rings of **10** are tilted by 10.2°, nearly the same as for **9**. The exocyclic Cp(C)–N bonds (1.400(3) Å) of **10** are significantly shorter than the N–CH<sub>3</sub> bonds (1.453(3) Å). Therefore, the exocyclic C–N bonds of **11** have partial double-bond character which is analogous to the partial double-bond character of the exocyclic B–N bonds of **9**.

We have prepared a sample of **10** using Plenio's procedure.<sup>18</sup> At 25 °C the  $^1\text{H}$  NMR and  $^{13}\text{C}$  NMR spectra each show a single signal for the CH(Cp) groups. Since these groups are crystallographically nonequivalent, conformational exchange is rapid on the NMR time scale. When the temperature is brought to –60 °C, the Cp(CH) signal separates into two peaks at  $\delta$  81.6 and 80.6, with  $\Delta G^\ddagger = 10.0$  kcal/mol. Although it is assumed that conformational exchanges are analogous, the boratabenzene complex has a 7 kcal/mol higher barrier. Since the major difference between the structures of **9** and **15** is the exocyclic B–N  $\pi$  bond for **9** and exocyclic C–N  $\pi$  bond of **15**, the difference seems to be due to the higher barriers to rotation about the B–N  $\pi$  bonds of **9**.



A final comparison may be made between the dimethylethylenediamino-bridged boratabenzene complex **8** and the corresponding bridged 3,3',4,4'-tetraphenylzirconocene dichloride **11**, which was also prepared by Plenio.<sup>17</sup> Regrettably the crystal structure has not been determined for **11**. The close analogy between the structures of the iron complexes **9** and **10** suggests that the structures of zirconium complexes **8** and **11** are similarly related. There are several available structures of dialkylamino zirconocenes which show short exocyclic Cp(C)–N distances, as expected for C–N  $\pi$  bonding.<sup>25–27</sup> Thus, the structure of **11** must incorporate exocyclic C–N  $\pi$  bonds.

A sample of **11** was prepared using Plenio's procedure.<sup>17</sup> At 25 °C the  $^1\text{H}$  NMR and  $^{13}\text{C}$  NMR spectra each show single peaks for the CH(Cp) groups. When the temperature is lowered to 10 °C, the  $^{13}\text{C}$  NMR signal separates into two peaks at  $\delta$  93.4 and 91.0. Coalescence at this temperature gives  $\Delta G^\ddagger = 13.0 \pm 0.5$  kcal/mol. We assume that the equilibration process for **11** is analogous to that illustrated in Figure 2 for **8**. The major component of the barrier to conformation interconversion in **11** would be rotation about the exocyclic Cp(C)–N  $\pi$ -bond. A recent measurement of a similar C–N bond rotation in the unbridged *meso*-bis(1-phenyl-3-pyrrolidyl)cyclopentadienylzirconium dichloride **16** gave a barrier of  $\Delta G^\ddagger = 12.1 \pm 0.2$  kcal/mol at –25 °C.<sup>27</sup> Thus, our assignment seems plausible.

## Conclusions

The comparison of the conformational barriers for the analogous Cp vs boratabenzene zirconium dichloride complexes **11** vs **8** shows that the boratabenzene com-

(25) For titanocenes, see: (a) Stahl, K.-P.; Boche, G.; Massa, W. J. *Organomet. Chem.* **1984**, 277, 113. (b) However, note: Carter, C. A. G.; McDonald, R.; Stryker, J. M. *Organometallics* **1999**, 18, 820.

(26) (a) Barsties, E.; Schaible, S.; Proscenc, M.-H.; Rief, U.; Röhl, W.; Weyand, O.; Dorer, B.; Brintzinger, H. H. *J. Organomet. Chem.* **1996**, 520, 63. (b) Luttikhedde, H. J. G.; Leino, R. P.; Wilén, C.-E.; Näsman, J. H.; Ahlgrén, M. J.; Pakkanen, T. A. *Organometallics* **1996**, 15, 3092.

(27) Knüppel, S.; Fauré, J.-L.; Erker, G.; Kehr, G.; Nissinen, M.; Fröhlich, R. *Organometallics* **2000**, 19, 1262.

plex has an 8.3 kcal/mol higher barrier. This difference appears to be due to the stronger B–N  $\pi$ -bonding of **8** relative to the weaker C–N  $\pi$ -bonding of **11**. Prior work on olefin polymerization catalysts derived from boratabenzene zirconium complexes, e.g. **2**, has emphasized the ability of boron to interact with B-bound donor substituents.<sup>14,15</sup> It had been assumed that similar interaction was less important for Cp–Zr complexes. The comparison of **11** with **8** demonstrates the greater B–N  $\pi$  interaction and provides its first quantitative measure.

Finally it should be noted that the  $C_2$  chirality of **8** is due solely to the conformational properties of the dimethylethylenediamino bridge. The high barrier to interconversion implies the enantiomeric conformers are relatively long-lived. Chiral  $C_2$ -symmetric bridged group 4 metallocenes have found extensive use as stereoselective catalysts for the polymerization of  $\alpha$ -olefins. Unfortunately the chiral bridge of **8** is to the rear of the open metal wedge, while the front edge of the wedge appears highly symmetrical. Therefore, we remain pessimistic about the use of **8** itself as a stereoselective catalyst. However, ring-substituted derivatives of **8** which have greater steric differentiation in the front of the metal wedge seem more promising candidates for stereoselective catalysts.

### Experimental Section

**General Remarks.** All reactions were carried out under an atmosphere of argon or nitrogen. Solvents were dried using standard procedures. The mass spectra were determined using a VG-70-S spectrometer. The NMR spectra were obtained using either a Bruker WH 400, WH 300, or AM 300 spectrometer. The <sup>1</sup>H NMR spectra and <sup>13</sup>C NMR spectra were calibrated by using signals from solvents referenced to Me<sub>4</sub>Si. The <sup>11</sup>B NMR spectra were referenced to external BF<sub>3</sub>·OEt<sub>2</sub>. The combustion analyses were determined by the analytical service department of the Department of Chemistry, The University of Michigan.

*N,N*-Bis(trimethylsilyl)-*N,N*-dimethylethylene-1,2-diamine,<sup>19</sup> 1-chloro-1-boracyclohexa-2,5-diene,<sup>28</sup> [2,5-diazahexane-2,5-diylbis(3,4-diphenylcyclopentadienyl)]iron(II),<sup>18</sup> and [2,5-diazahexane-2,5-diylbis(3,4-diphenylcyclopentadienyl)]zirconium(IV) dichloride<sup>17</sup> were prepared by literature procedures. All other compounds are commercially available.

***N,N*-Bis(1-boracyclohexadienyl)-*N,N*-dimethylethylene-1,2-diamine (**13**).** A solution of 1.33 g (5.73 mmol) of *N,N*-bis(trimethylsilyl)-*N,N*-dimethylethylene-1,2-diamine in 10 mL of pentane was added to a solution of 1.29 g (11.5 mmol) of 1-chloro-1-boracyclohexa-2,5-diene in 15 mL of pentane at –78 °C. The color changed to yellow, and a white precipitate formed. The reaction mixture was stirred at –78 °C for 2 h and warmed to 25 °C with stirring for 10 h. All volatile components were removed in vacuo, leaving an oily semicrystalline mixture (1.29 g, 96%). The <sup>1</sup>H NMR spectrum was consistent with the product being a mixture of double-bond isomers. <sup>11</sup>B NMR (155 MHz, C<sub>6</sub>D<sub>6</sub>):  $\delta$  39.6, 31.9. HRMS (EI): calcd for C<sub>14</sub>H<sub>22</sub><sup>11</sup>B<sub>2</sub>N<sub>2</sub>(M), 240.1969; found, 240.1960.

**Lithium *N,N*-Bis(1-boratabenzene)-*N,N*-dimethylethylene-1,2-diamine (**14**).** A solution of **3** (1.27 g, 5.29 mmol) was dissolved in 4 mL of THF and added to a solution of LDA (1.24 g, 2.2 equiv) in 5 mL of THF at –78 °C. The color of the solution turned to dark red. The mixture was stirred at –78 °C for 2 h and then warmed to 25 °C for 10 h. The volatile components were removed in vacuo, and the residue was

**Table 3. Crystal Data and Structure Refinement Details for **8** and **9****

	<b>8</b>	<b>9</b>
empirical formula	C <sub>14</sub> H <sub>20</sub> B <sub>2</sub> Cl <sub>2</sub> N <sub>2</sub> Zr	C <sub>14</sub> H <sub>20</sub> B <sub>2</sub> FeN <sub>2</sub>
fw	400.06	293.79
temp, K	158(2)	158(2)
wavelength, Å	0.710 73	0.710 73
cryst syst	triclinic	orthorhombic
space group	$P\bar{1}$ (No. 2)	$Pna2_1$ (No. 33)
unit cell dimens		
<i>a</i> , Å	9.1808(2)	16.3330(1)
<i>b</i> , Å	9.7105(2)	6.5780(2)
<i>c</i> , Å	11.1676(1)	12.4488(2)
$\alpha$ , deg	65.234(1)	
$\beta$ , deg	79.177(1)	
$\gamma$ , deg	64.270(1)	
<i>V</i> , Å <sup>3</sup> ; <i>Z</i>	814.35(2); 2	1337.38(2); 4
calcd density, Mg/m <sup>3</sup>	1.632	1.459
abs coeff, mm <sup>-1</sup>	0.995	1.111
<i>F</i> (000)	404	616
cryst size, mm	0.30 × 0.28 × 0.03	0.12 × 0.16 × 0.18
limiting indices	–11 ≤ <i>h</i> ≤ 13, –11 ≤ <i>k</i> ≤ 12, 0 ≤ <i>l</i> ≤ 14	–21 ≤ <i>h</i> ≤ 21, –8 ≤ <i>k</i> ≤ 8, –16 ≤ <i>l</i> ≤ 11
no. of rflns collected	8461	12 787
no. of indep rflns	3577 ( <i>R</i> (int) = 0.0157)	3279 ( <i>R</i> (int) = 0.0841)
abs cor	semiempirical from equiv	semiempirical from equiv
refinement method	full-matrix least squares on <i>F</i> <sup>2</sup>	full-matrix least squares on <i>F</i> <sup>2</sup>
no. of data/restraints/ params	3575/0/270	3279/1/252
GOF on <i>F</i> <sup>2</sup>	1.120	1.018
final <i>R</i> indices	<i>R</i> 1 = 0.0238, w <i>R</i> 2 = 0.0552	<i>R</i> 1 = 0.0574, w <i>R</i> 2 = 0.1303
<i>R</i> indices (all data)	<i>R</i> 1 = 0.0266, w <i>R</i> 2 = 0.0562	<i>R</i> 1 = 0.0754, w <i>R</i> 2 = 0.1412
largest diff peak and hole, e/Å <sup>3</sup>	0.465 and –0.326	1.164 and –1.021

washed with 3 × 30 mL of pentane to give a pale yellow solid product which was dried in vacuo. Yield: 1.85 g, 89%). <sup>1</sup>H NMR (360 MHz, THF-*d*<sub>6</sub>):  $\delta$  6.97 (dd, *J* = 10.0, 6.6 Hz, H <sub>$\beta$</sub> , 4H); 5.72 (d, *J* = 10.0 Hz, H <sub>$\alpha$</sub> , 4H); 5.50 (t, *J* = 6.6 Hz, H <sub>$\gamma$</sub> , 2H); 3.60 (m, THF, 8H); 3.13 (s, NCH<sub>2</sub>, 4H); 2.75 (s, NCH<sub>3</sub>, 6H); 1.80 (m, THF, 8H). <sup>11</sup>B NMR (155 MHz, THF-*d*<sub>6</sub>):  $\delta$  37.6. <sup>13</sup>C NMR (90.5 MHz, THF-*d*<sub>6</sub>):  $\delta$  134.5 (C <sub>$\beta$</sub> ); 111.7 (C <sub>$\alpha$</sub> ); 101.7 (C <sub>$\gamma$</sub> ); 68.2 (THF); 51.9 (NCH<sub>2</sub>), 37.8 (NCH<sub>3</sub>), 26.3 (THF).

**[*N,N*-Bis(1-boratabenzene)-*N,N*-dimethylethylene-1,2-diamine]iron(II) (**9**).** Lithium salt **14** (1.0 g, 2.5 mmol) was dissolved in 6 mL of THF and added to a suspension of FeCl<sub>2</sub> (1.0 equiv) in 4 mL of THF at –78 °C. The mixture was stirred at –78 °C for 1 h and warmed to 25 °C for 10 h. The mixture then turned dark red. Insoluble materials were removed by filtration, and the volatiles were removed in vacuo, affording a dark red solid which was recrystallized from CH<sub>2</sub>-Cl<sub>2</sub>/pentane to afford 280 mg (38%) of product, mp 162 °C dec. <sup>1</sup>H NMR (360 MHz, C<sub>6</sub>D<sub>6</sub>):  $\delta$  4.74 (m, H <sub>$\beta$</sub> , 4H); 4.62 (d, *J* = 11.8 Hz, H <sub>$\alpha$</sub> , 2H); 4.55 (t, *J* = 6.0 Hz, H <sub>$\gamma$</sub> , 2H); 4.37 (m, H <sub>$\alpha'$</sub> , 2H); 3.44 (d, *J* = 8.0 Hz, NCH<sub>2</sub>, 2H); 3.02 (s, NCH<sub>3</sub>, 6H); 2.80 (d, *J* = 8.0 Hz, NCH<sub>2</sub>', 2H). <sup>11</sup>B NMR (115 MHz, C<sub>6</sub>D<sub>6</sub>):  $\delta$  19.7. <sup>13</sup>C NMR (100.6 MHz, C<sub>6</sub>D<sub>6</sub>):  $\delta$  92.1 (C <sub>$\beta$</sub> ); 89.4 (C <sub>$\beta$</sub> '); 73.9 (br, C <sub>$\alpha$</sub> ); 71.6 (C <sub>$\gamma$</sub> ); 65.9 (C <sub>$\alpha'$</sub> ); 51.5 (NCH<sub>3</sub>); 38.6 (NCH<sub>2</sub>). When the temperature was raised, the signals at  $\delta$  92.1 and 89.4 collapsed to a single peak at  $\delta$  92.5; *T*<sub>c</sub> = 75 °C. HRMS (EI, *m/z*): calcd for C<sub>14</sub>H<sub>20</sub><sup>11</sup>B<sub>2</sub><sup>56</sup>FeN<sub>2</sub> (M), 294.1162; found, 294.1159. Anal. Calcd for C<sub>14</sub>H<sub>20</sub>B<sub>2</sub>FeN<sub>2</sub>: C, 57.24; H, 6.86; N, 9.54. Found; C, 56.77; H, 6.78; N, 9.32.

**[*N,N*-Bis(1-boratabenzene)-*N,N*-dimethylethylene-1,2-diamine]zirconium(IV) Dichloride (**8**).** Lithium salt **14** (0.65 g, 2.70 mmol) was dissolved in 10 mL of ether, which was added to a suspension of 0.65 g (2.80 mmol) of ZrCl<sub>4</sub> in ether at –78 °C. The mixture was stirred at –78 °C for 12 h

(28) Maier, G.; Henkelmann, X.; Reisenauer, H. P. *Angew. Chem., Int. Ed. Engl.* **1985**, *24*, 1065.

and then warmed to 25 °C. Removal of solvent left a red residue which was taken up in toluene. Recrystallization afforded 150 mg (14%) of product, mp 214 °C. <sup>1</sup>H NMR (400 MHz, C<sub>6</sub>D<sub>6</sub>): δ 2.24 (m, NCH, 2H); 3.51 (m, NCH', 2H); 2.48 (s, NCH<sub>3</sub>, 6H); 4.82 (ddd, *J* = 10.8, 5.4, 1.8 Hz, H<sub>α</sub>, 2H); 5.73 (ddd, *J* = 10.8, 5.4, 1.8 Hz, H<sub>α</sub>', 2H); 6.38 (t, *J* = 6.8 Hz, H<sub>γ</sub>, 2H); 6.93 (ddd, *J* = 10.8, 6.7, 1.8 Hz, H<sub>β</sub>, 2H); 7.75 (ddd, *J* = 10.8, 6.7, 1.8 Hz, H<sub>β</sub>', 2H). <sup>11</sup>B NMR (115 MHz, C<sub>6</sub>D<sub>6</sub>): δ 31.5. <sup>13</sup>C NMR (100.6 MHz, C<sub>6</sub>D<sub>6</sub>): δ 37.3 (NCH<sub>3</sub>); 50.4 (NCH<sub>2</sub>); 112.0 (C<sub>γ</sub>); 142.2 (C<sub>β</sub>); 154.2 (C<sub>β</sub>'); C<sub>α</sub> not observed. HRMS (EI): calcd for C<sub>14</sub>H<sub>20</sub><sup>11</sup>B<sub>2</sub><sup>35</sup>Cl<sub>2</sub>N<sub>2</sub><sup>90</sup>Zr, 398.0237; found, 398.0229. Anal. Calcd for C<sub>14</sub>H<sub>20</sub>B<sub>2</sub>Cl<sub>2</sub>N<sub>2</sub>Zr: C, 42.02; H, 5.05; N, 7.0. Found: C, 42.68; H, 5.06; N, 6.96.

**Measurement of the Conformational Equilibrium of 8.** The <sup>1</sup>H NOESY experiment was run on a dilute solution of **8** in C<sub>6</sub>D<sub>6</sub> at 400 MHz with a relaxation time of 6 s and mixing times of 3.5 and 4.5 s at 318 K. The signals at δ 7.75 and 6.93 and at δ 5.73 and 4.82 showed large positive cross-peaks. The rates were calculated by assuming an equally populated two-site exchange, employing the equation  $k = 1/t_m \ln[(a_d + a_x)/(a_d - a_x)]$ , where *t<sub>m</sub>* = mixing time and *a<sub>d</sub>* and *a<sub>x</sub>* are the diagonal and cross-peak volumes in arbitrary units. Eight independent measurements gave  $k = 0.0169(15) \text{ s}^{-1}$ .

**Variable-Temperature <sup>13</sup>C NMR Spectra of 10 and 11.** Complexes **10** and **11** were prepared as described by Plenio et

al.<sup>17,18</sup> The NMR spectra were consistent with those described in the original literature. When a sample of **10** in CDCl<sub>3</sub> was cooled, the signal for Cp(CH) at δ 81.4 separated into two peaks at δ 81.6 and 80.6 (*T<sub>c</sub>* = -60 °C). When a sample of **11** in CDCl<sub>3</sub> was cooled, the signal for Cp(CH) at δ 92.2 separated into two peaks at δ 93.4 and 91.0 (*T<sub>c</sub>* = 10 °C).

**X-ray Structure Determinations.** Crystals of **8** and **9** suitable for X-ray diffraction were obtained by recrystallization from toluene and pentane/CH<sub>2</sub>Cl<sub>2</sub>, respectively. Crystallographic data are collected in Table 3. ORTEP drawings of **8** and **9** showing the numbering schemes used in the refinements are illustrated in Figures 1 and 3, respectively. Additional crystallographic data are available in the Supporting Information.

**Acknowledgment.** We are grateful to the National Science Foundation and the Dow Chemical Company for financial assistance.

**Supporting Information Available:** Details of the X-ray crystallographic studies of **8** and **9**. This material is available free of charge via the Internet at <http://pubs.acs.org>.

OM000861G